

The influence of PBAT content in the nanocapsules preparation and its effect in essential oils release

Rennan Felix da Silva Barbosa ^a, Alana Gabrieli de Souza ^a, Vijaya Rangari ^b,
Derval dos Santos Rosa ^{a,*}

^a Centro de Engenharia, Modelagem e Ciências Sociais Aplicadas – CECS/Universidade Federal do ABC (UFABC) – Santo André, Avenida dos Estados, 5001, CEP: 09210-580, SP, Brazil

^b Department of Materials Science and Engineering, Tuskegee University, Tuskegee, AL 36088, USA

ARTICLE INFO

Keywords:

Essential oil
Biodegradable nanocapsules
Polymeric wall
Poly(butylene adipate-co-terephthalate)

ABSTRACT

Nanoencapsulation provides new alternatives for the food industry, enabling a controlled and slow release of active antimicrobial agents, such as essential oils (EO). Poly (butylene adipate-co-terephthalate) (PBAT) nanocapsules loaded with linalool EO were prepared using an extrusion method with 1, 3, and 5% w/v (PBAT to chloroform). Nanocapsules' sizes ranged from 100 to 250 nm and were spherical. The release profile was studied using an ethanoic medium over 24 h, and according to the Korsmeyer-Peppas model, a Fick diffusion mechanism was involved. FT-IR and thermogravimetric analyses confirmed EO encapsulation with an encapsulation efficiency of 55%, 71%, and 74% for 1, 3, and 5%, respectively. The results indicated that encapsulation depended on organic phase concentration, with higher PBAT contents achieving better results. The resulting nanocapsules had antimicrobial activity against *E. coli*, which could be extended to develop active packaging systems.

1. Introduction

Biodegradable polymers are promising materials for the development of new sustainable products due to their environmentally friendly characteristics. These types of material can be used for packaging, films, and membranes, and their biodegradable nature would reduce the amounts of wastes associated with food packaging. Antimicrobial active agents may be incorporated into packages to improve food quality, shelf life, safety, and integrity (Espitia & Otoni, 2018). Natural materials have attracted considerable attention due to their efficiency and low toxicity, including essential oils (EO), which are recognized as possessing antimicrobial and antifungal properties (Shetta, Kegere, & MAMDouh, 2019; Šožić et al., 2018).

However, EO present some application challenges because they present high volatility, low water solubility, and oxidation susceptibility (Liu et al., 2017; Zanetti et al., 2018). The nanoencapsulation is a promising method to overcome the EO limitations since this process avoids unwanted reactions with media, masks odors and flavors, and protect EO against possible oxidations, moisture, and heat (de Matos et al., 2019; Rao, Chen, & McClements, 2019; Van de Vel, Sampers, & Raes, 2019). Antonioli et al. prepared PLA nanocapsules loaded with

lemongrass essential oil and reported excellent protection against volatilization (Antonioli et al., 2020). Besides, encapsulation reduces the migration rate of active compounds material to the external environment (Wen et al., 2016).

The nanoencapsulation is a promising way to develop an active system for incorporation into packaging since it does not affect polymers' transparency. Also, greater encapsulation efficiency can be attained due to higher surface area at the nanoscale (Rao & Geckeler, 2011; dos Santos et al., 2016). Different wall materials are used to develop nanocapsules, such as chitosan, alginate, polylactic acid, and others (Natrajan et al., 2015; Quesada, Sendra, Navarro, & Sayas-Barberá, 2016; Sun et al., 2017; Wu et al., 2016). However, most of them show low encapsulation efficiency and large particle size (Lee, Yun, & Park, 2016; dos Santos et al., 2016). Thus, new alternatives have been sought, and the use of new biodegradable materials to produce polymeric nanocapsules have attracted attention (dos Santos et al., 2016).

In this work, we have developed innovative biodegradable nanocapsules by using Poly (butylene adipate-co-terephthalate) – PBAT polymer. The capsules were prepared by the extrusion method and loaded with Linalool essential oil, which is known for its antimicrobial activity. There are no studies in the literature that present the use of the

* Corresponding author.

E-mail address: derval.rosa@ufabc.edu.br (D.S. Rosa).

PBAT as an encapsulating agent. The loading of EO and their controlled release, chemical, thermal, dimensional (i.e., sizes), and morphological properties were studied.

2. Materials and methods

2.1. Materials

BASF (Ludwigshafen, Germany) supplied Poly(butylene adipate-co-terephthalate) (PBAT), with a molar mass of 66,500 g mol⁻¹. Linalool essential oil was provided by Quinaris (Ponta Grossa, PR, Brazil). Chloroform, Polysorbate 80 (Tween 80), Ethanol, and Mueller-Hinton agar (KASVI) were purchased from Sigma-Aldrich (São Paulo, SP, Brazil), and used as received. Distilled water was used in all formulations.

2.2. Capsules preparation

PBAT was dissolved in chloroform to prepare an organic polymer solution by magnetic stirring (Fisatom model 753A, São Paulo, SP, Brazil) for 4 h. Based on the literature, three different polymeric concentrations were used: 1, 3, and 5% w/v (Antonioli et al., 2020; Pina-Barrera et al., 2019). Then 300 µl of EO was mixed with 100 mg of polysorbate 80 in 100 mL of water and stirred for 30 min.

The prepared PBAT solution was added into the EO aqueous solution using a syringe (diameter of 0.3 µm) at 0.2 mL per minute, using a peristaltic pump (Variable-Flow Peristaltic Pumps, Fisher Scientific, Hampton, United States). This mixture was stirred for 24 h. Capsules were separated from the solution through centrifugation at 15,000 rpm (Thermo Scientific 75,002,426 – Thermo Fisher Scientific, Massachusetts, USA), and were then washed with water and centrifuged again at 15,000 rpm. Capsules were dried at room temperature, weighted, and stored in a glass bottle in the refrigerator.

2.3. Dynamic light scattering (DLS) and static light scattering (SLS)

DLS and SLS tests were performed on an equipment ALV-CGS3 (ALV-GmbH, Langen, Germany) at a fixed angle of 90°. Polarized HeNe laser was used (22 mW), with a wavelength of 633 nm, and a pair of APD detectors operating in pseudo-correlation. The samples were previously ultrasonicated for 3 min in a VCX-750 (Sonics & Materials, Newtown, United States). The tests were conducted in triplicate.

2.4. Transmission electron microscopy (TEM)

The nanocapsules microstructure and morphology were investigated using a Transmission Electron Microscope, Model JEM2010 (JEOL, Tokyo, Japan). The dried nanocapsules were re-dispersed in an aqueous solution (0.1 wt%), and a solution drop was deposited on a copper grid for analysis. The capsules nanosizes were measured using ImageJ software, and 25 capsules were used to calculate the nanocapsules' diameter.

2.5. Thermogravimetric analysis and encapsulation efficiency (EE %)

TGA tests were conducted using STA 6000 (TA Instruments, New Castle, United States), under an N₂ atmosphere, in a flow rate of 50 mL min⁻¹, at a heating rate of 10 °C min⁻¹, and a temperature range of 30–600 °C.

The oil loading was measured evaluating the weight loss assigned to the EO according to

Eq. (1):

$$OL(\%) = \frac{w_o - w_f}{w_o} \quad (1)$$

where OL (%) is the loaded oil on nanocapsules, w_f and w_o are the final and initial weight of capsules, respectively.

The encapsulation efficiency was calculated by the ratio of OL (%), and capsules' yield (Y) to the total oil (TO) used, as presented in Eq. (2)

$$EE(\%) = \frac{OL \times Y}{TO} \quad (2)$$

2.6. Essential oil release

The release mechanism was evaluated by the dried capsules addition in ethanoic medium (50% ethanol and 50% water) to stimulate the encapsulated EO liberation. This system was used as it is a simulant in food applications. Samples were evaluated in a Cary 50 UV-VIS spectrophotometer (Agilent, Santa Clara, United States), at a wavelength of 207 nm (Jabir, Taha, & Sahib, 2018; Jabir et al., 2019). The measurements were carried out in triplicate and followed for 24 h.

The data were fitted with the Korsmeyer-Peppas model, using Eq. (3):

$$\frac{M_t}{M_\infty} = K \cdot t^n \quad (3)$$

where $\frac{M_t}{M_\infty}$ is a fraction of EO released at time t, K is the release rate constant, and n is the release exponent (Wu, Bala, Škalko-Basnet, & di Cagno, 2019).

2.7. Fourier transform infrared spectroscopy

FTIR analysis was performed on a VARIAN 66 spectrophotometer (PerkinElmer, Waltham, United States), in the range 4000–600 cm⁻¹, 64 scans, and spectral resolution of 1 cm⁻¹. The capsules were dried at room temperature in a desiccator, and then the ATR accessory was used to record the FTIR spectra.

2.8. Antimicrobial activity

The microbiological test was carried out to evaluate the capsules' potential application. For that, 100 mg of capsules were placed in inoculated Petri dishes. Then, a nutrient agar culture medium, Mueller-Hinton agar (KASVI), was added and inoculated with *Escherichia coli* bacteria suspension with a count of 10⁵ colony-forming unit (CFU) mL⁻¹. After 48 h of inoculation, in a microbiological oven at 37 °C, the inhibition radius was analyzed to evaluate the biocidal effect. The tests were conducted in triplicate.

2.9. Statistical analysis

The experimental results were subjected to variance analysis (One-way ANOVA) to evaluate the concentration effect on capsules diameter. The mean values were considered to be significantly different at 95% confidence level ($p \leq 0.05$).

3. Results and discussions

3.1. Nanocapsules formation and dimensional evaluation

The essential oil (EO) retention inside a material core depends on several variables and is associated with EO's chemical nature (i.e., chemical functionality and active groups), polarity, molecular mass, and the wall material properties (Assadpour & Mahdi Jafari, 2019; Ju et al., 2019). The EO hydrophobic character affects the encapsulation process, and surfactants allow a hydrophilic-hydrophobic balance to improve encapsulation efficiency (Pavoni, Perinelli, Bonacucina, Cespi, & Palmieri, 2020). Tween 80 is a conventional surfactant that reduces interfacial/surface tension between two adjacent fluids (Han et al., 2018; Prakash et al., 2019). Its use above the critical micellar concentration in

the EO-water mixture results in a stable emulsion with micelles, where the hydrophobic surfactant group interacts with the EO (Mendes et al., 2020; Ryu, Corradini, McClements, & McLandsborough, 2019). After the micelle formation, the polymeric solution addition disturbs the system, and the PBAT chains coat the micelles and form the biodegradable nanocapsules. The expected capsules and their respective interactions are shown in Fig. 1, which illustrates the coated micelles.

The nanospheres were evaluated by the DLS technique (Bhattacharjee, 2016), and Fig. 2 presents the capsules hydrodynamic radius (R_H). The curves showed two distinct peaks: the first one showed an R_H average of ~ 4 nm and the second of ~ 160 nm. This behavior may be associated with two systems present in the medium: the micelles and the nanocapsules.

The first peak indicates that, probably, some micelles were not coated and did not form nanocapsules, i.e., the encapsulation was not wholly efficient (the yield of capsules formation is presented in Section 3.3). The second peak is related to polymeric clusters, i.e., nanospheres, and the peaks differences are associated with the capsule's preparation steps, as illustrated in Fig. 2(a) and (b). The peaks observed in DLS analysis are shown in Fig. 2(c).

The nanocapsules were obtained by polymer interfacial deposition through a syringe, with the organics' solution added to the aqueous phase. The surfactant and essential oil micelles provide a region for droplet precipitation in the solution. As the solvent evaporates from the system, a polymer sphere is formed around the micelles (Fig. 2b). Besides, considering the different PBAT contents of 1, 3, and 5%, the samples showed nanometric R_H values of 170, 232, 157 nm, respectively.

Complementary to DLS analysis, the SLS allows the evaluation of particles' shape using the gyration radius (R_G), which analyzes the weight averaged root mean square distance from the samples' center of mass (Burchard, 2003; Xu, 2015). As stated by Kassalainen et al., R_G is more sensitive to the particle structure and geometry than the R_H (Kaasalainen et al., 2017). An analysis of the formed structure can be obtained by the R_G/R_H ratio, where values of 0.775, ~ 1 , 1.78, and >2 of R_G have been reported for hard spheres, hollow spheres, random coils, and rod-like structures, respectively (Burchard, 2003). In this work, all the systems presented R_G of ~ 0.7 , indicating that they are organized in spheres and that are not hollow spheres, i.e. indicating that the EO was trapped inside these structures.

3.2. Transmission electron microscopy

Fig. 3 shows TEM photomicrographs of EO-surfactant micelles and

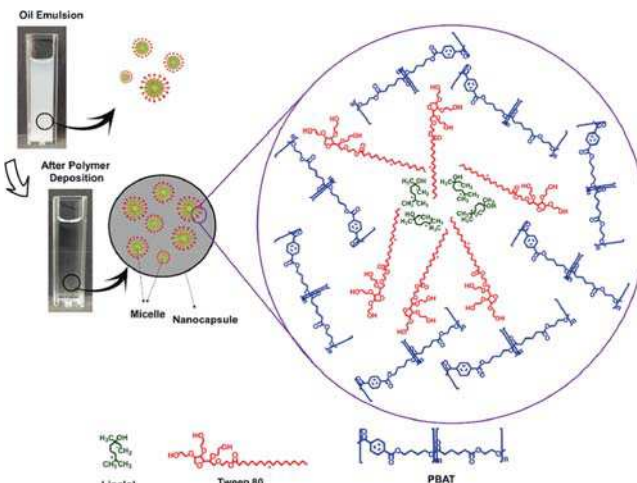


Fig. 1. Illustration of the nanocapsules and structural arrangement of compounds.

nanocapsules prepared with 1, 3, and 5% PBAT. Fig. 3(a) shows surfactant-EO micelles that presented a spherical shape and 9.2 ± 1.5 nm diameter, being within the range observed in DLS analysis.

From Fig. 3(b)–(d), capsules presented mean diameters of 134.7 ± 28.9 , 133.6 ± 24.3 , 234.6 ± 29.6 nm, for 1, 3, and 5% PBAT, respectively. One-Way ANOVA was applied to evaluate the capsules size statistically, and the Tukey test was conducted to confirm the similarity between samples. The system without PBAT addition (emulsion) was different from all systems, confirming the polymers' effect in the emulsion to form nanocapsules. Systems with 1 and 3% PBAT were statistically similar, indicating that both concentrations generate capsules with similar size; in this case, it is more interesting the 3% concentration, considering the higher yield. However, capsules using 1 and 3% presented an asymmetric shape, that could impact capsules stability and efficiency. The system with 5% PBAT was statistically different from other samples and presented a regular spherical shape, indicating that 5% was the best condition to prepare PBAT nanocapsules. The observed dimensions agreed with DLS and SLS analysis.

3.3. Thermogravimetric analysis

Fig. 4(a) shows PBAT, essential oil, and nanocapsules thermograms. The EO presents a single thermal event associated with its evaporation, starting at 62°C and having maximum evaporation at 140°C , as can be observed by the derivative thermogravimetry (DTG) curve (Fig. 4(b)). This thermal behavior confirms EO's high volatility and justifies its encapsulation (Xiao, Xu, & Zhu, 2017).

Pristine PBAT showed a single degradation event, with T_{onset} and T_{max} values of $\sim 330^\circ\text{C}$ and 401°C , respectively, associated with the polymer chains scission in random regions that starts in the interface between adipic acid and 1,4-butanediol (Felipe Jaramillo et al., 2019). Because of its high thermal stability, PBAT has excellent potential as a wall material in capsules systems.

Nanocapsules presented a similar mass loss event than the neat PBAT, associated with the wall material (Barbosa, Souza, & Rosa, 2020). However, a new thermal event in lower temperatures was verified and is associated with the EO trapped inside the capsule structure. This thermal event induced a weight loss of 7.1, 9.5, and 11.3 wt% for nanocapsules with PBAT concentration of 1, 3, and 5%, respectively, and indicates that the encapsulation process of linalool EO using PBAT was successful.

The thermal event associated with the encapsulated EO was used to estimate the encapsulation efficiency by the ratio of encapsulated EO regarding the EO used during the process (Antonioli et al., 2020; Silva, Caldera, Trotta, Nerín, & Domingues, 2019). As Bastos et al. presented, the EO weight percentage inside capsules can be used alongside the nanocapsules yield to calculate the encapsulation efficiency (Eq. (2)) (Bastos et al., 2020). The measured EE% was 55, 71, and 74% for 1, 3, and 5% PBAT samples, respectively. These values are similar to recent literature and highlight the PBAT potential as wall material (Hasani, Ojagh, & Ghorbani, 2018). The low EE (%) obtained for 1% PBAT was due to the lower yield, and these values are affected by the molecular mass of the polymer, the interaction between the components of the system, and the method used to obtain the capsules (Saifullah et al., 2019).

3.4. Essential oil release

Innumerable mechanisms can describe the encapsulated EO release after its encapsulation with different materials (Duman & Kaya, 2016). The release medium is associated with simulant of food systems, as presented in EU regulation (European Commission, 2011, 2017), and the most common is the ethanoic medium. Fig. 4(c) shows the nanocapsules time-dependent release profiles in an ethanoic medium (50%). The differences observed in EO release can be attributed to the EE% of each formulation. The profile for 1% and 3% is quite similar, and a

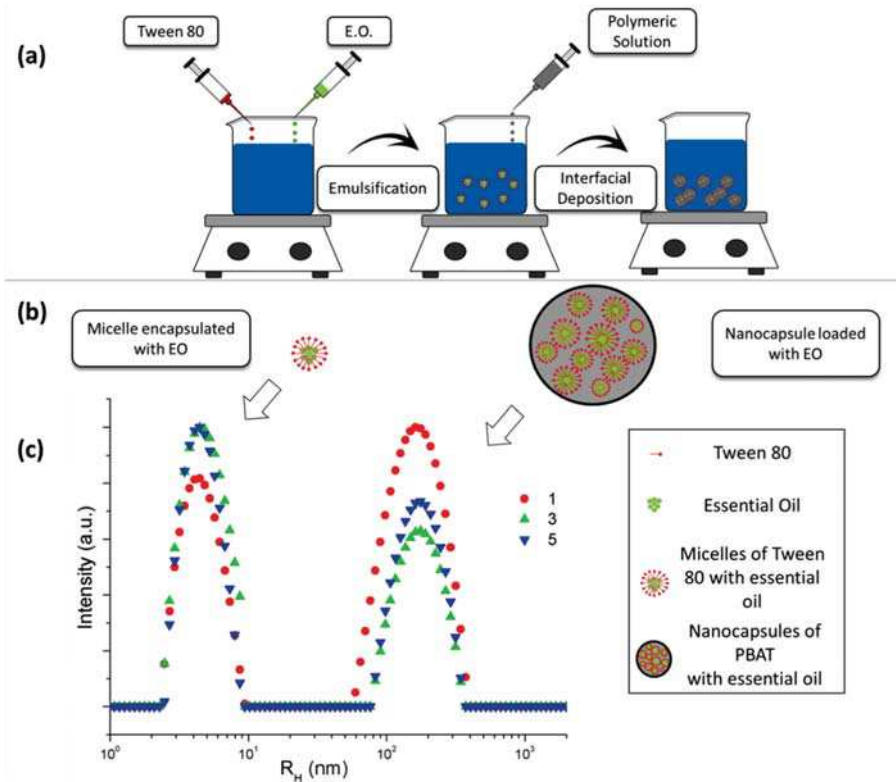


Fig. 2. (a) Methodology schematic illustration, (b) Oil encapsulation process according to the method step, and (c) Nanocapsules DLS results.

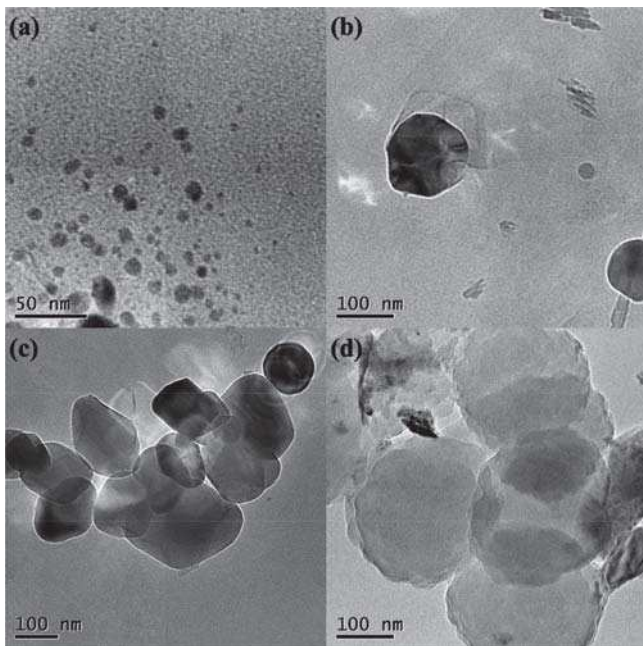


Fig. 3. Transmission electron microscopy images for (a) emulsion showing micelles, (b) nanocapsules of PBAT at 1%, (c) nanocapsules of PBAT at 3%, and (d) nanocapsules of PBAT at 5%.

slower release profile is observed for nanocapsules prepared with 5%; this difference is associated with the polymeric layer thickness and capsules dimensions and shapes.

For the model used to evaluate the data (Korsmeyer-Peppas), the 'n' values indicate the release mechanism involved. For $n < 0.43$, Fickian diffusion (case I transport) dominates the system; if $0.43 < n < 0.85$, it

indicates non-Fickian or anomalous transport, and $n > 0.85$ corresponds to zero-order release kinetics (case II transport) (Dima, Pătrașcu, Cantaragi, Alexe, & Dima, 2016). The log cumulative percentage release plot versus log time obtained the following n values: $n = 0.23, 0.34$, and 0.43 for 1%, 3%, and 5%, respectively.

The obtained curve can be separated into two stages. The first one shows a rapid EO release, where $\sim 50\%$ of the release occurred in the first stage; this behavior resulted from a high oil content attached to the internal surface of capsules and their swelling degree (Hasani et al., 2018). At the contact with the solvent solution, it penetrates the material wall, and the polymer passes from a glassy to a rubbery state. Over the swelling stage, in the polymer coexist inside a glassy state and outside a rubbery state (Maderuelo, Zarzuelo, & Lanao, 2011). In these conditions, the release rate depends simultaneously on the swelling and the diffusion process (Dima et al., 2016). A slow-release rate characterizes the second phase until a constant value is achieved (plateau). There was no significant difference between the samples release profile after 24 h.

The encapsulated oil delivery mechanism is associated with: i) adsorbed oil in lower concentrations, on the surface of the capsules, occupying small porosities and defects, and ii) loosened inside the capsule. When adding the capsules in an ethanoic environment, the oil that occupied the pores and interstices possibly leaves the capsules more quickly, resulting in a faster release profile. The oil inside the capsules depends on diffusion mechanisms, characterizing a slower release profile (i.e., achieved plateau).

The nanocapsules' thickness was calculated in ImageJ software, and the observed values were 8, 9, and 15 nm for samples 1, 3, and 5%, respectively. According to Cuomo et al. (2014), the amount of retained oil and the release curves are related to the wall thickness (Cuomo et al., 2014). The essential oil apparent diffusion coefficients (D_{app}) were calculated following the Eq. (4), according to the model used for Cuomo et al. 2015 (Cuomo et al., 2015), where h is the wall thickness, and C/C_0 indicates the fraction of oil released at time t .

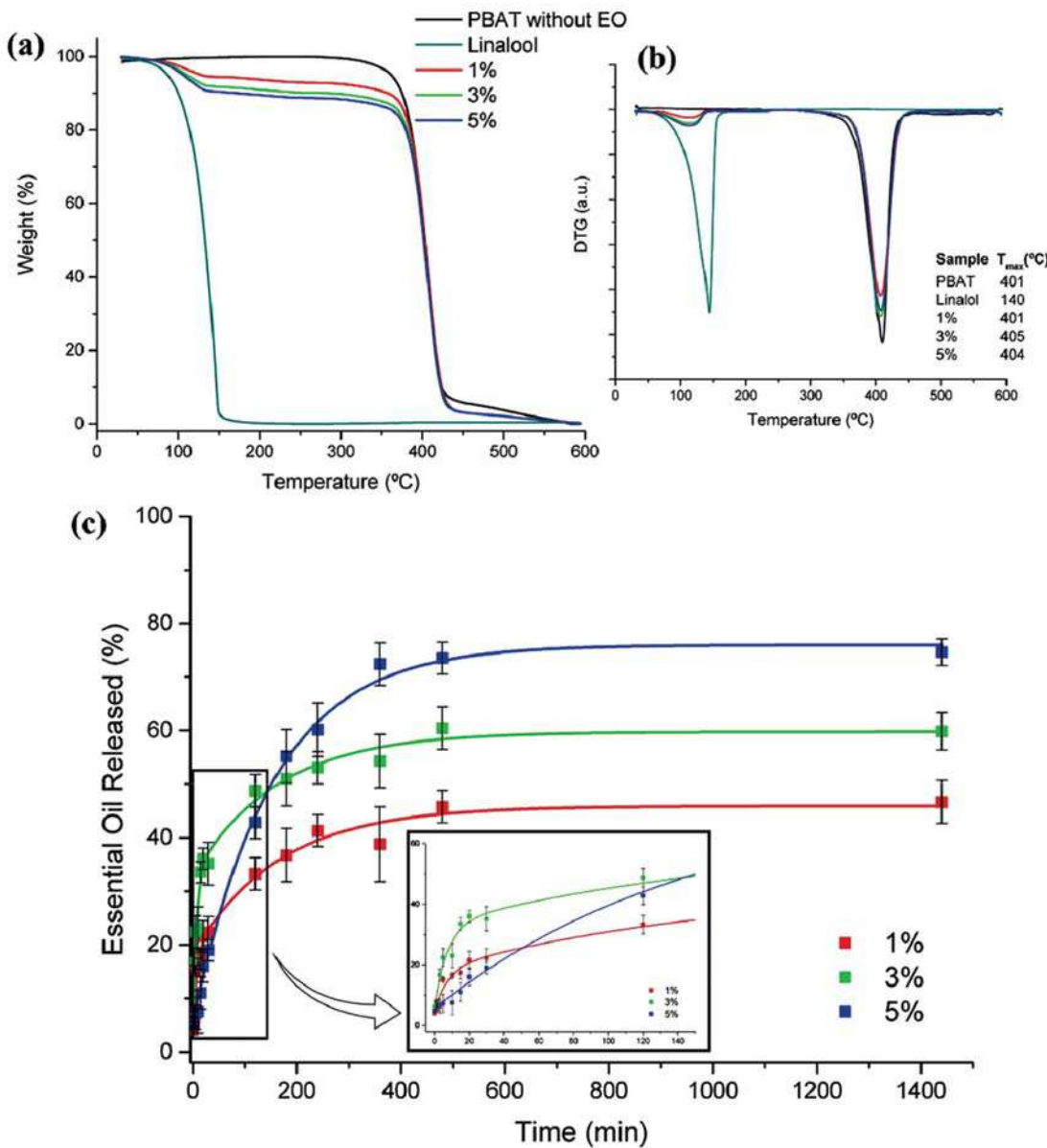


Fig. 4. Thermogravimetric curves of neat PBAT, Essential Oil, and Nanocapsules containing EO and using PBAT as wall material with concentrations of 1, 3, and 5%: (a) TGA and (b) DTG, and (c) release profile of essential oil from nanocapsules with the different polymeric solutions.

$$\frac{C}{C_0} = 4 \left(\frac{D_{app} \cdot t}{\pi \cdot h^2} \right)^{0.5} \quad (4)$$

The observed values were 1.12×10^{-9} , 1.04×10^{-9} , and 7.33×10^{-10} $\text{cm}^2 \text{s}^{-1}$, for samples 1, 3, and 5%, respectively. These results show that the higher thickness provides a barrier that slows the oil diffusion through the nanocapsules. Considering the release profiles, n , and D_{app} values and the TEM images, higher PBAT contents in the organic phase resulted in larger wall thickness and lower permeability of the capsules, which implies low diffusion coefficients and promotes slower oil release, which is the objective of this work.

3.5. Chemical structure evaluation

The PBAT FTIR spectrum is presented in Fig. 5(a), and its IR peaks were observed at 3065, 2958, 2875, 1710, 1410, 1366, 1267, and 726 cm^{-1} , assigned as the = C—H absorption in stretching mode; CH_3 and

CH_2 stretch; C=O bond of ester groups; angular deformation of the $-\text{CH}_2-$ bond; C—O group; and off-plane benzene ring deformations, respectively (Barbosa et al., 2020; Black-Solis et al., 2019; Hernández-López et al., 2019; Li et al., 2018). The other raw materials used were Tween 80 and Linalool, and their spectra are presented in Fig. 5(a).

The Tween 80 characteristic peaks are found at 3462 cm^{-1} (O—H stretching vibrations), 2938 and 2869 cm^{-1} (asymmetric and symmetric stretching vibrations of methylene ($-\text{CH}_2-$)), 1730 cm^{-1} (C=O stretching of the ester group), and the absorption lines in the range 850–1100 cm^{-1} refer to the polyoxyethylene chain of the surfactant (Krstonović et al., 2019). The EO spectrum showed large bands at 3420, 2979, and 2920 cm^{-1} ; the peaks at 1644, 1450, 1114, 1000, and 691 cm^{-1} were attributed to C=C group, (C—H) vibrations, secondary alcohol group (C—O), C—O stretching band, and aromatic compound C—H group, respectively (Jabir et al., 2018; Xiao et al., 2017).

Fig. 5(b) shows the nanocapsules FTIR spectra, and all samples showed similar peaks to the neat PBAT structure, which is the wall

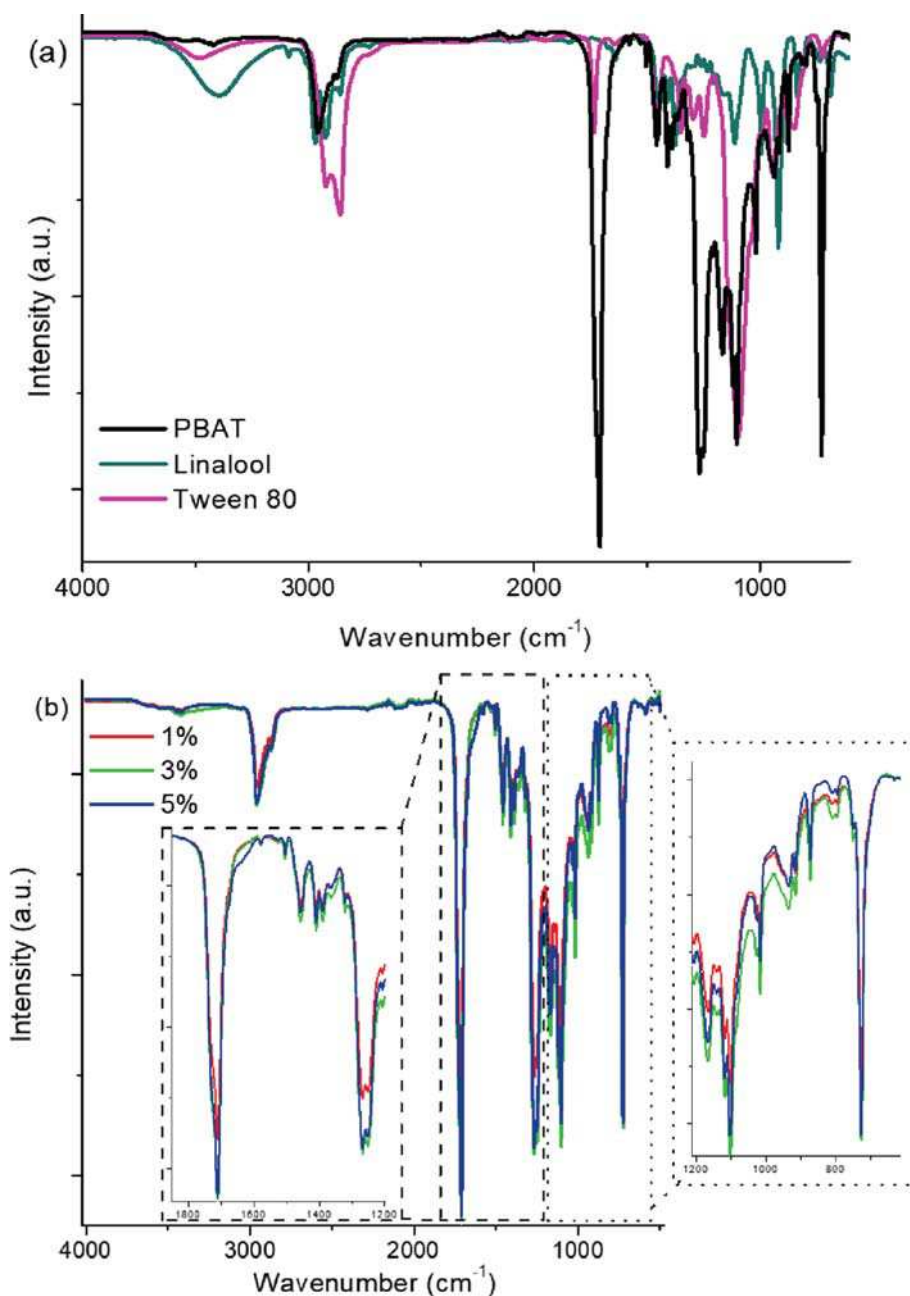


Fig. 5. FTIR spectra of (a) raw materials used in the production of nanocapsules (PBAT, Linalool essential oil, and Tween 80 – surfactant) and (b) nanocapsules with different PBAT contents and zoom of the main peaks.

material (Y. Zhang et al., 2019). Only slight spectral changes were observed, such as shoulders at ~ 1624 and ~ 1080 cm^{-1} , especially for the 5% sample. The absence of EO peaks is attributed to the good encapsulation efficiency, indicating the surfactant and oil absence in the external capsules' surface.

3.6. Antimicrobial activity

The disc diffusion assay was performed against *E. coli* to evaluate the capsules' effectiveness against microorganisms. *E. coli* is a Gram-negative bacterium with an outer membrane containing lipopolysaccharides that may protect the bacteria from active compounds and impose a challenge for its control (Chu et al., 2019). The microbiological test was carried out with the 5% PBAT capsules, and Fig. 6 shows the obtained results.

A region without bacterial growth is observed, known as the

inhibition zone, with a diameter of 55 mm. Literature usually reports inhibition halos in the range of 20 to 50 mm, highlighting the developed capsules' antimicrobial potential (Amor et al., 2019; Santos et al., 2019). Linalool EO acts by changing the bacterium cell structure permeability and electron transport, impacting the DNA and cell metabolism and leading to *E. coli* inhibition growth or death (Gao et al., 2019). In this work, the developed capsules showed great activity against *E. coli*, which is considered a high resistance microorganism, indicating that our capsules can be suitable against other bacteria, especially against Gram-positive. These observations point out that the developed capsules present potential as active antimicrobial agents to incorporate food packaging.

3.7. Final remarks

Recent authors highlighted the continuous search for new strategies

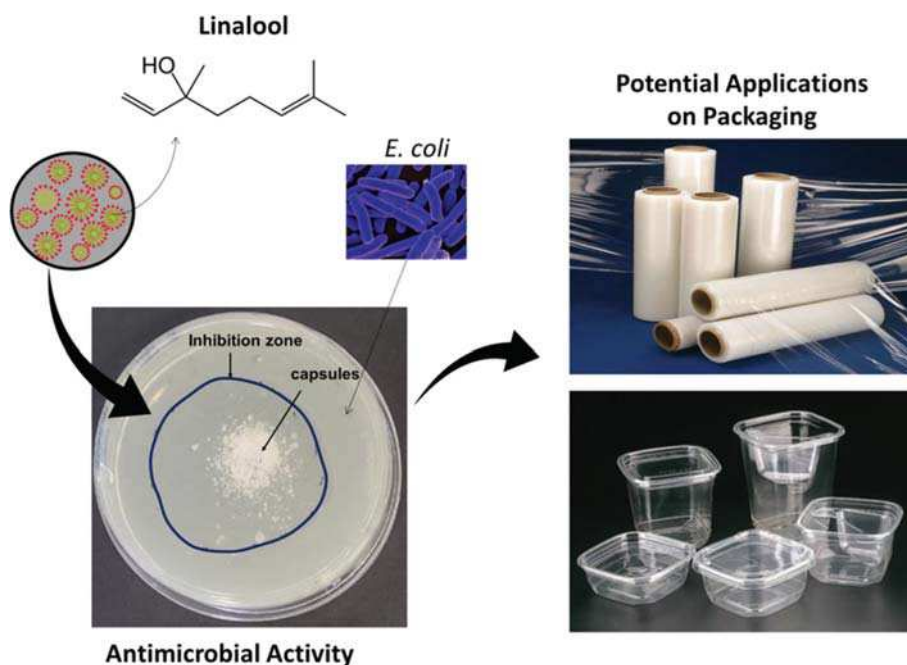


Fig. 6. Result of the antimicrobial test of 5% PBAT capsules of Linalool essential oil, highlighting the inhibition zone and potential use on packaging.

to enhance food product shelf life, and the development of active packaging or food additives shows promising perspectives (Assadpour & Mahdi Jafari, 2019; Giannakas et al., 2019). Among the existent additives, essential oils are natural molecules with good antimicrobial potential, which could slow the food spoilage and improve the food shelf life (Rezaei et al., 2019). However, EO needs to be protected from thermal and oxidation degradation (Shetta et al., 2019). In this scenario, nanoencapsulation have been gaining interest as it provides a greater loading capacity and encapsulation efficiency, stability, and controlled release of encapsulated material (Antonioli et al., 2020; Gaber Ahmed, González, & Díaz García, 2020; He et al., 2019). Nanocapsules are easy to apply and can be introduced in several food applications, avoiding pathogenic microbial contamination and guaranteeing food safety and quality (He et al., 2019; Pavoni et al., 2020).

This work aimed to prepare PBAT nanocapsules with antimicrobial activity to cover nanocapsule application possibilities in the food sector (Fukushima, Rasyida, & Yang, 2013; Rahimi, Aeinehvand, Kim, & Otaigbe, 2017). Since PBAT is a biodegradable and biocompatible polymer, its use is considered safe for food contact. Other biodegradable polymeric materials like polylactic acid and polycaprolactone have been reported as excellent materials for the encapsulation of essential oils (Modaresifar, Azizian, & Hadjizadeh, 2016; Stramarkou, Oikonomopoulou, Missirli, Thanassoulia, & Krokida, 2020). As PBAT presents similar characteristics, it may present potential as additive material that can extend shelf life by controlled delivery of encapsulated essential oil. However, its use in nanoencapsulation was not exploited yet, since no works in the literature reported the PBAT capsules production.

Several authors used the encapsulation approach for food technologies, aiming to extend the food shelf life. Antonioli demonstrated that lemongrass essential oil nanocapsules were highly effective against *C. gloeosporioides*, even at low concentrations (Antonioli et al., 2020). These results indicate that nanocapsules are an excellent option for preventing apple fungi contamination and reducing the fruits rot lesions and necrotic effects. Froio et al. observed that bergamot and orange essential oil encapsulated into polymer nanoparticles presented great antimicrobial activity in active packaging formulation (Froio et al., 2019). The authors reported that the nanocapsules are excellent options to prolong the orange juice shelf life.

Zhang et al. reported the use of nanoencapsulated tarragon essential

oil, using chitosan–gelatin as coating materials, and studied its use as pork slices coating, showing that the encapsulated EO is advantageous over the use of free EO, allowing a prolonged storage time and improving sensory attributed (Zhang, Liang, Li, & Kang, 2020). In addition to countless others cited in the present work, these works highlight the importance of nanocapsules containing active compounds in the food area, either directly in the food or in packaging. Based on that, this work developed PBAT capsules for the first time and demonstrated that these have the potential to be applied in active packaging due to their physicochemical characteristics, slow-release, and antimicrobial properties.

4. Conclusions

PBAT nanocapsules loaded with EO were successfully prepared. The nanocapsules sizes ranged from 100 to 250 nm and presented spherical shape. The organic phase concentration resulted in different capsules' size distribution and homogeneity. These slight changes in the morphology can be attributed to the high PBAT contents in the solution and the interactions between the three components: polymer, surfactant, and EO. Encapsulation was verified by thermal analysis, and the encapsulation efficiency was 55%, 71%, and 74% for samples using 1, 3, and 5 w/v PBAT, respectively. The release profile was mathematically adjusted according to the Korsmeyer-Peppas model, where it was observed that the release mechanism is associated with a Fickian diffusion process. The capsules retained the EO during 24 h in ethanol, with a rapid release at the start, attributed to the high oil content attached to the capsules surface, and showed that the EO release depends simultaneously by the swelling and the diffusion processes. Higher polymer contents in the organic phase resulted in a proportionally larger wall thickness that resulted in a higher concentration of oil encapsulated in the polymer structure, thus improving encapsulation efficiency. The thicker the nanocapsule, the lower the permeability and slower the oil delivery due to the difficulty of its diffusion through the polymer wall, which highlights the capsules developed using 5% PBAT. The Fourier transform infrared spectroscopy (FT-IR) confirmed the EO encapsulation. Capsules presented great antimicrobial activity against *E. coli*, highlighting the use of PBAT as wall material for EO's encapsulation. These observations could expand the application of PBAT and

broaden the use of essential oils as possible additives in the food industry package.

Declaration of Competing Interest

The authors declare that they have no known competing financial interests or personal relationships that could have appeared to influence the work reported in this paper.

Acknowledgments

The authors thank the financial support provided by FAPESP (2018/11277-7, and 2018/25239-0), CAPES (Code 001), NSF-CREST #1735971, and the Multiuser Experimental Center of the Federal University of ABC (CEM-UFABC).

References

Amor, G., Caputo, L., La Storia, A., De Feo, V., Mauriello, G., & Fechtali, T. (2019). Chemical composition and antimicrobial activity of artemisia herba-alba and origanum majorana essential oils from Morocco. *Molecules*, 24(22). <https://doi.org/10.3390/molecules24224021>.

Antonioli, G., Fontanella, G., Echeverrigaray, S., Longaray Delamare, A. P., Fernandes Pauletti, G., & Barcellos, T. (2020). Poly(lactic acid) nanocapsules containing lemongrass essential oil for postharvest decay control: In vitro and in vivo evaluation against phytopathogenic fungi. *Food Chemistry*, 326(May), Article 126997. <https://doi.org/10.1016/j.foodchem.2020.126997>.

Assadpour, E., & Mahdi Jafari, S. (2019). A systematic review on nanoencapsulation of food bioactive ingredients and nutraceuticals by various nanocarriers. *Critical Reviews in Food Science and Nutrition*, 59(19), 3129–3151. <https://doi.org/10.1080/10408398.2018.1484687>.

Barbosa, R. F. S., Souza, A. G., & Rosa, D. S. (2020). Acetylated cellulose nanostructures as reinforcement materials for PBAT nanocomposites. *Polymer Composites*, 18–21. <https://doi.org/10.1002/pc.25580>.

Bastos, L. P. H., Vicente, J., Santos, C. H. C., Carvalho, M. G. de, & Garcia-Rojas, E. E. (2020). Encapsulation of black pepper (*Piper nigrum* L.) essential oil with gelatin and sodium alginate by complex coacervation. *Food Hydrocolloids*, 102(September 2019). <https://doi.org/10.1016/j.foodhyd.2019.105605>.

Bhattacharjee, S. (2016). DLS and zeta potential – What they are and what they are not? *Journal of Controlled Release*, 235, 337–351. <https://doi.org/10.1016/j.jconrel.2016.06.017>.

Black-Solis, J., Ventura-Aguilar, R. I., Correa-Pacheco, Z., Corona-Rangel, M. L., & Bautista-Baños, S. (2019). Preharvest use of biodegradable polyester nets added with cinnamon essential oil and the effect on the storage life of tomatoes and the development of *Alternaria alternata*. *Scientia Horticulturae*, 245(October 2018), 65–73. <https://doi.org/10.1016/j.scienta.2018.10.004>.

Burchard, W. (2003). Solubility and solution structure of cellulose derivatives. *Cellulose*, 10(3), 213–225. <https://doi.org/10.1023/A:1025160620576>.

Chu, Y., Xu, T., Gao, C. C., Liu, X., Zhang, N., Feng, X., ... Tang, X. (2019). Evaluations of physicochemical and biological properties of pullulan-based films incorporated with cinnamon essential oil and Tween 80. *International Journal of Biological Macromolecules*, 122, 388–394. <https://doi.org/10.1016/j.ijbiomac.2018.10.194>.

Cuomo, F., Ceglie, A., Pilidu, M., Miguel, M. G., Lindman, B., & Lopez, F. (2014). Loading and protection of hydrophilic molecules into liposome-templated polyelectrolyte nanocapsules. *Langmuir*, 30(27), 7993–7999. <https://doi.org/10.1021/la501978u>.

Cuomo, F., Lopez, F., Pilidu, M., Miguel, M. G., Lindman, B., & Ceglie, A. (2015). Release of small hydrophilic molecules from polyelectrolyte capsules: Effect of the wall thickness. *Journal of Colloid and Interface Science*, 447(1), 211–216. <https://doi.org/10.1016/j.jcis.2014.10.060>.

Dima, C., Petrușcu, L., Cantaragi, A., Alexe, P., & Dima, S. (2016). The kinetics of the swelling process and the release mechanisms of *Coriandrum sativum* L. essential oil from chitosan/alginate/inulin microcapsules. *Food Chemistry*, 195, 39–48. <https://doi.org/10.1016/j.foodchem.2015.05.044>.

Duman, F., & Kaya, M. (2016). Crayfish chitosan for microencapsulation of coriander (*Coriandrum sativum* L.) essential oil. *International Journal of Biological Macromolecules*, 92, 125–133. <https://doi.org/10.1016/j.ijbiomac.2016.06.068>.

Espitia, P. J. P., & Otoni, C. G. (2018). Nanotechnology and edible films for food packaging applications. *Bio-Based Materials for Food Packaging*, 125–145. https://doi.org/10.1007/978-981-13-1909-9_6.

European Commission. (2011). Commission Regulation (EU) No 10/2011. Official Journal of the European Union, (L 12), 1–89.

European Commission. (2017). Regulation (EU) 2017/752. Official Journal of the European Union, 2017(L 113), 18–23.

Felipe Jaramillo, A., Riquelme, S., Montoya, L. F., Sánchez-Sanhueza, G., Medinam, C., Rojas, D., ... Francisco Meléndrez, M. (2019). Influence of the concentration of copper nanoparticles on the thermo-mechanical and antibacterial properties of nanocomposites based on Poly (butylene adipate-co-terephthalate). *Polymer Composites*, 40(5), 1870–1882. <https://doi.org/10.1002/pc.24949>.

Froio, F., Ginot, L., Paolino, D., Lebaz, N., Bentaher, A., Fessi, H., & Elaissari, A. (2019). Essential oils-loaded polymer particles: Preparation, characterization and antimicrobial property. *Polymers*, 11(6). <https://doi.org/10.3390/polym11061017>.

Fukushima, K., Rasyida, A., & Yang, M. C. (2013). Characterization, degradation and biocompatibility of PBAT based nanocomposites. *Applied Clay Science*, 80–81, 291–298. <https://doi.org/10.1016/j.clay.2013.04.015>.

Gaber Ahmed, G. H., González, A. F., & Díaz García, M. E. (2020). Nano-encapsulation of grape and apple pomace phenolic extract in chitosan and soy protein via nanoemulsification. *Food Hydrocolloids*, 105806. <https://doi.org/10.1016/j.foodhyd.2020.105806>.

Gao, Z., Van Nostrand, J. D., Zhou, J., Zhong, W., Chen, K., & Guo, J. (2019). Anti-listeria activities of linalool and its mechanism revealed by comparative transcriptome analysis. *Frontiers in Microbiology*, 10. <https://doi.org/10.3389/fmicb.2019.02947>.

Giannakas, A., Salmas, C., Leontiou, A., Tsimogiannis, D., Oreopoulos, A., & Braouli, J. (2019). Novel LDPE/chitosan rosemary and melissa extract nanostructured active packaging films. *Nanomaterials*, 9(8). <https://doi.org/10.3390/nano9081105>.

Han, Y., Yu, M., & Wang, L. (2018). Physical and antimicrobial properties of sodium alginate/carboxymethyl cellulose films incorporated with cinnamon essential oil. *Food Packaging and Shelf Life*, 15(October 2017), 35–42. <https://doi.org/10.1016/j.fpsl.2017.11.001>.

Hasani, S., Ojagh, S. M., & Ghorbani, M. (2018). Nanoencapsulation of lemon essential oil in Chitosan-Hicap system. Part 1: Study on its physical and structural characteristics. *International Journal of Biological Macromolecules*, 115, 143–151. <https://doi.org/10.1016/j.ijbiomac.2018.04.038>.

He, X., Deng, H., & Hwang, H. min. (2019). The current application of nanotechnology in food and agriculture. *Journal of Food and Drug Analysis*, 27(1), 1–21. <https://doi.org/10.1016/j.jfda.2018.12.002>.

Hernández-López, M., Correa-Pacheco, Z. N., Bautista-Baños, S., Zavaleta-Avejar, L., Benítez-Jiménez, J. J., Sabino-Gutiérrez, M. A., & Ortega-Gudiño, P. (2019). Bio-based composite fibers from pine essential oil and PLA/PBAT polymer blend. Morphological, physicochemical, thermal and mechanical characterization. *Materials Chemistry and Physics*, 234(October 2018), 345–353. <https://doi.org/10.1016/j.matchemphys.2019.01.034>.

Jabir, M. S., Taha, A. A., & Sahib, S. (2018). Antioxidant activity of Linalool. *Engineering and Technology Journal*, 36(1B), 64–67. <https://doi.org/10.30684/etj.36.1B.11>.

Jabir, Majid S., Taha, A. A., Sahib, U. I., Tagi, Z. J., Al-Shammari, A. M., & Salman, A. S. (2019). Novel of nano delivery system for Linalool loaded on gold nanoparticles conjugated with CALNN peptide for application in drug uptake and induction of cell death on breast cancer cell line. *Materials Science and Engineering C*, 94(March 2018), 949–964. <https://doi.org/10.1016/j.msec.2018.10.014>.

Ju, J., Chen, X., Xie, Y., Yu, H., Guo, Y., Cheng, Y., ... Yao, W. (2019). Application of essential oil as a sustained release preparation in food packaging. *Trends in Food Science and Technology*, 92(1800), 22–32. <https://doi.org/10.1016/j.tifs.2019.08.005>.

Kaasalainen, M., Aseyev, V., von Haartman, E., Karaman, D.Ş., Mäkilä, E., Tenhu, H., ... Salonen, J. (2017). Size, stability, and porosity of mesoporous nanoparticles characterized with light scattering. *Nanoscale Research Letters*, 12(1). <https://doi.org/10.1186/s11671-017-1853-y>.

Krstonić, V., Milanović, M., & Đokić, L. (2019). Food Hydrocolloids Application of different techniques in the determination of xanthan gum- SDS and xanthan gum-Tween 80 interaction. *Food Hydrocolloids*, 87(April 2018), 108–118. <https://doi.org/10.1016/j.foodhyd.2018.07.040>.

Lee, B. K., Yun, Y., & Park, K. (2016). PLA micro- and nanoparticles. *Advanced Drug Delivery Reviews*, 107, 176–191. <https://doi.org/10.1016/j.addr.2016.05.020>.

Li, X., Tan, D., Xie, L., Sun, H., Sun, S., Zhong, G., & Ren, P. (2018). Effect of surface property of halloysite on the crystallization behavior of PBAT. *Applied Clay Science*, 157, 218–226. <https://doi.org/10.1016/j.clay.2018.02.005>.

Liu, Y., Wang, S., Zhang, R., Lan, W., & Qin, W. (2017). Development of Poly (lactic acid)/ Chitosan Fibers Loaded with Essential Oil for Antimicrobial Applications. <https://doi.org/10.3390/nano7070194>.

Maderuelo, C., Zarzuelo, A., & Lanza, J. M. (2011). Critical factors in the release of drugs from sustained release hydrophilic matrices. *Journal of Controlled Release*, 154(1), 2–19. <https://doi.org/10.1016/j.jconrel.2011.04.002>.

Matos, S. P. de, Lucca, L. G., & Koester, L. S. (2019). Essential oils in nanostructured systems: Challenges in preparation and analytical methods. *Talanta*, 195(July 2018), 204–214. <https://doi.org/10.1016/j.talanta.2018.11.029>.

Mendes, J. F., Norcino, L. B., Martins, H. H. A., Manrich, A., Otoni, C. G., Carvalho, E. E. N., ... Mattoso, L. H. C. (2020). Correlating emulsion characteristics with the properties of active starch films loaded with lemongrass essential oil. *Food Hydrocolloids*, 100, 105428–105439. <https://doi.org/10.1016/j.foodhyd.2019.105428>.

Modaresifar, K., Azizian, S., & Hadjizadeh, A. (2016). Nano/biomimetic tissue adhesives development: From research to clinical application. *Polymer Reviews*, 56(2), 329–361. <https://doi.org/10.1080/15583724.2015.1114493>.

Natrajan, D., Srinivasan, S., Sundar, K., & Ravindran, A. (2015). Science direct formulation of essential oil-loaded chitosan e alginate nanoparticles. *Journal of Food and Drug Analysis*, 23(3), 560–568. <https://doi.org/10.1016/j.jfda.2015.01.001>.

Pavoni, L., Perinelli, D. R., Bonacucina, G., Cespi, M., & Palmieri, G. F. (2020). An overview of micro-and nanoemulsions as vehicles for essential oils: Formulation, preparation and stability. *Nanomaterials*, 10(1). <https://doi.org/10.3390/nano10010135>.

Pina-Barrera, A. M., Alvarez-Roman, R., Baez-Gonzalez, J. G., Amaya-Guerra, C. A., Rivas-Morales, C., Gallardo-Rivera, C. T., & Galindo-Rodriguez, S. A. (2019). Application of a multisystem coating based on polymeric nanocapsules containing essential oil of Thymus vulgaris L. To increase the shelf life of table grapes (*Vitis*

Vinifera L.). *IEEE Transactions on Nanobioscience*, 18(4), 549–557. <https://doi.org/10.1109/TNB.2019.2941931>.

Prakash, A., Vadivel, V., Rubini, D., & Nithyanand, P. (2019). Antibacterial and antibiofilm activities of linalool nanoemulsions against *Salmonella Typhimurium*. *Food Bioscience*, 28(May 2018), 57–65. <https://doi.org/10.1016/j.fbio.2019.01.018>.

Quesada, J., Sendra, E., Navarro, C., & Sayas-Barberá, E. (2016). Antimicrobial active packaging including chitosan films with *Thymus vulgaris* L Essential Oil for Ready-to-Eat Meat. *Foods*, 5(3), 57. <https://doi.org/10.3390/foods5030057>.

Rahimi, S. K., Aeinehvand, R., Kim, K., & Otaigbe, J. U. (2017). Structure and biocompatibility of bioabsorbable nanocomposites of aliphatic-aromatic copolyester and cellulose nanocrystals. *Biomacromolecules*, 18(7), 2179–2194. <https://doi.org/10.1021/acs.biomac.7b00578>.

Rao, J., Chen, B., & McClements, D. J. (2019). Improving the efficacy of essential oils as antimicrobials in foods: Mechanisms of action. *Annual Review of Food Science and Technology*, 10(1), 365–387. <https://doi.org/10.1146/annurev-food-032818-121727>.

Rao, J. P., & Geckeler, K. E. (2011). Progress in polymer science polymer nanoparticles: Preparation techniques and size-control parameters. *Progress in Polymer Science*, 36 (7), 887–913. <https://doi.org/10.1016/j.progpolymsci.2011.01.001>.

Rezaei, A., Fathi, M., & Jafari, S. M. (2019). Nanoencapsulation of hydrophobic and low-soluble food bioactive compounds within different nanocarriers. *Food Hydrocolloids*, 88(June 2018), 146–162. <https://doi.org/10.1016/j.foodhyd.2018.10.003>.

Ryu, V., Corradini, M. G., McClements, D. J., & McLandsborough, L. (2019). Impact of ripening inhibitors on molecular transport of antimicrobial components from essential oil nanoemulsions. *Journal of Colloid and Interface Science*, 556, 568–576. <https://doi.org/10.1016/j.jcis.2019.08.059>.

Saifullah, M., Shishir, M. R. I., Ferdowsi, R., Tanver Rahman, M. R., & Van Vuong, Q. (2019). Micro and nano encapsulation, retention and controlled release of flavor and aroma compounds: A critical review. *Trends in Food Science and Technology*, 86 (December 2017), 230–251. <https://doi.org/10.1016/j.tifs.2019.02.030>.

Santos, J. D. C., Coelho, E., Silva, R., Passos, C. P., Teixeira, P., Henriques, I., & Coimbra, M. A. (2019). Chemical composition and antimicrobial activity of *Satureja montana* byproducts essential oils. *Industrial Crops and Products*, 137, 541–548. <https://doi.org/10.1016/j.indcrop.2019.05.058>.

Santos, P. P. dos P. P. dos;, Oliveira, A. De, Pereira, P., Hickmann, S., Flôres, S. H., Rios, A. de O., & Chisté, R. C. (2016). Biodegradable polymers as wall materials to the synthesis of bioactive compound nanocapsules. *Trends in Food Science & Technology*, 53, 23–33. <https://doi.org/10.1016/j.tifs.2016.05.005>.

Shettha, A., Kegere, J., & Mamdouh, W. (2019). Comparative study of encapsulated peppermint and green tea essential oils in chitosan nanoparticles: Encapsulation, thermal stability, in-vitro release, antioxidant and antibacterial activities. *International Journal of Biological Macromolecules*, 126, 731–742. <https://doi.org/10.1016/j.ijbiomac.2018.12.161>.

Silva, F., Caldera, F., Trotta, F., Nerín, C., & Domingues, F. C. (2019). Encapsulation of coriander essential oil in cyclodextrin nanosponges: A new strategy to promote its use in controlled-release active packaging. *Innovative Food Science and Emerging Technologies*, 56, Article 102177. <https://doi.org/10.1016/j.ifset.2019.102177>.

Šojoć, B., Pavlić, B., Tomović, V., Ikonić, P., Zeković, Z., Kocić-tanackov, S., ... Ivić, M. (2018). University of Novi Sad , Faculty of Technology , Bulevar cara Lazara University of Novi Sad , Institute of Food Technology , Bulevar cara University of Belgrade , Institute of General and Physical Chemistry , Food Chemistry, (2019). <https://doi.org/10.1016/j.foodchem.2018.12.137>.

Stramarkou, M., Oikonomopoulou, V., Missirli, T., Thanassoulia, I., & Krokida, M. (2020). Encapsulation of rosemary essential oil into biodegradable polymers for application in crop management. *Journal of Polymers and the Environment*, 28(8), 2161–2177. <https://doi.org/10.1007/s10924-020-01760-5>.

Sun, L., Sun, J., Chen, L., Niu, P., Yang, X., & Guo, Y. (2017). Preparation and characterization of chitosan film incorporated with thinned young apple polyphenols as an active packaging material. *Carbohydrate Polymers*, 163, 81–91. <https://doi.org/10.1016/j.carbpol.2017.01.016>.

Van de Vel, E., Sampers, I., & Raes, K. (2019). A review on influencing factors on the minimum inhibitory concentration of essential oils. *Critical Reviews in Food Science and Nutrition*, 59(3), 357–378. <https://doi.org/10.1080/10408398.2017.1371112>.

Wen, P., Zhu, D. H., Wu, H., Zong, M. H., Jing, Y. R., & Han, S. Y. (2016). Encapsulation of cinnamon essential oil in electrospun nanofibrous film for active food packaging. *Food Control*, 59, 366–376. <https://doi.org/10.1016/j.foodcont.2015.06.005>.

Wu, H., Hu, W., Zhang, Y., Huang, L., Zhang, J., Tan, S., ... Liao, X. (2016). Effect of oil extraction on properties of spent coffee ground-plastic composites. *Journal of Materials Science*, 51(22), 10205–10214. <https://doi.org/10.1007/s10853-016-0248-2>.

Wu, I. Y., Bala, S., Škalko-Basnet, N., & di Cagno, M. P. (2019). Interpreting non-linear drug diffusion data: Utilizing Korsmeyer-Peppas model to study drug release from liposomes. *European Journal of Pharmaceutical Sciences*, 138, Article 105026. <https://doi.org/10.1016/j.ejps.2019.105026>.

Xiao, Z., Xu, Z., & Zhu, G. (2017). Production and characterization of nanocapsules encapsulated Linalool by ionic gelation method using chitosan as wall material. *Food Science and Technology*, 37(4), 613–619. <https://doi.org/10.1590/1678-457x.27616>.

Xu, R. (2015). Light scattering: A review of particle characterization applications. *Particuology*, 18, 11–21. <https://doi.org/10.1016/j.partic.2014.05.002>.

Zanetti, M., Carniel, T. K., Dalcanton, F., dos Anjos, R. S., Gracher Riella, H., de Araújo, P. H. H., ... Antônio Fiori, M. (2018). Use of encapsulated natural compounds as antimicrobial additives in food packaging: A brief review. *Trends in Food Science and Technology*, 81, 51–60. <https://doi.org/10.1016/j.tifs.2018.09.003>.

Zhang, H., Liang, Y., Li, X., & Kang, H. (2020). Effect of chitosan-gelatin coating containing nano-encapsulated tarragon essential oil on the preservation of pork slices. *Meat Science*, 166, Article 108137. <https://doi.org/10.1016/j.meatsci.2020.108137>.

Zhang, Y., Jiang, Z., Zhang, Z., Ding, Y., Yu, Q., & Li, Y. (2019). Polysaccharide assisted microencapsulation for volatile phase change materials with a fluorescent retention indicator. *Chemical Engineering Journal*, 359, 1234–1243. <https://doi.org/10.1016/j.cej.2018.11.054>.